Quantum point contact conductance in normal-metal/insulator/metal/superconductor junctions

William J. Herrera,* J. Virgilio Niño,† and J. Jairo Giraldo‡
Departamento de Física, Universidad Nacional de Colombia, Bogotá, Colombia
(Received 12 June 2004; revised manuscript received 14 October 2004; published 29 March 2005)

The effect of an insulating barrier located at a distance a from a *NS* quantum point contact is analyzed in this work. The Bogoliubov-de Gennes equations are solved for *NINS* junctions (*S*, anisotropic superconductor; *I*, insulator; and *N*, normal metal), where the *NIN* region is a quantum wire. For $a\neq 0$, quasibound states and resonances in the differential conductance are predicted. These resonances depend on the symmetry of the pair potential, the strength of the insulating barrier and a. Our results show that in a *NINS* quantum point contact the number of resonances vary with the symmetry of the order parameter. This is to be contrasted with the results for the *NINS* junction, in which only the position of the resonances changes with the symmetry.

DOI: 10.1103/PhysRevB.71.094515 PACS number(s): 74.20.Rp, 74.50.+r, 74.45.+c, 81.07.Lk

I. INTRODUCTION

In high critical temperature superconductivity the symmetry of the pair potential is one of the most studied aspects.[1,2] Tunneling spectra depend strongly on this symmetry and therefore tunneling spectroscopy is a very sensitive tool for its study. In a *d*-symmetry and (110) orientation, for instance, the differential conductance has a peak at zero voltage, called zero-bias conductance peak (ZBCP), which has been predicted theoretically by different authors.[3–8] and observed experimentally by others.[9–14] The existence of the ZBCP is due to the formation of Andreev quasibound states at the Fermi level (zero energy states) close to the interface.[15–17] These states appear by the interference between quasiparticles scattered at the interface because they can experience a different pair potential due to the superconductor anisotropy. Quantum point contacts studies in NIS junctions show that the ZBCP is removed by the quasiparticle diffractions at the point contact,[18,19] an aspect that has been shown experimentally.[14] In contrast, in quantum point contacts with *p*-superconductors, the ZBCP appears, even for single mode junctions.[20] Tunneling spectroscopy has been proposed to determine the parity of the pair potential.[20–22] Recently two quantum point contacts have been studied for the crossed Andreev reflection in *d*-wave superconductors.[23]

On the other hand, in *NINS* (Refs. 24 and 25) and *NISN* junctions,[26,27] resonances in the differential conductance appear. In anisotropic superconductors, the resonance energies depend on the symmetry of the pair potential. In *NINS* junctions and d_{xy}-symmetry the positions of these resonances are out of phase with respect to those predicted for isotropic superconductors.[28] In *NISN* junctions the conductance presents two types of resonances due to anisotropy of the pair potential.[27]

In this paper, we analyze the differential conductance when quasiparticles are injected into a superconductor from a single-mode quantum wire, with an insulating barrier located at a distance a of the *NS* interface (*NINS* quantum point contact). We show that there exist quasibound states which cause resonances in the differential conductance and that the number of these resonances depends on the symmetry of the order parameter. This is shown through the solution of the Bogoliubov-de Gennes equations in *NINS* junctions, where the *NIN* region is modeled by a wire of width W. In particular, *s*- and *d*-symmetries are considered.

II. THE BOGOLIUBOV-DE GENNES EQUATIONS AND THEIR SOLUTIONS IN *NINS* POINT CONTACTS

The elementary excitations or quasiparticles in a superconductor are described by the Bogoliubov-de Gennes (BdG) equations, which can be generalized for anisotropic superconductors.[29] For a steady state these equations are

$$\begin{aligned} H_e(\mathbf{r}_1)\tilde{u}(\mathbf{r}_1) + \int d\mathbf{r}_2\tilde{\Delta}(\mathbf{r}_1,\mathbf{r}_2)\tilde{v}(\mathbf{r}_2) &= E\tilde{u}(\mathbf{r}_1), \\ -H_e^*(\mathbf{r}_1)\tilde{v}(\mathbf{r}_1) + \int d\mathbf{r}_2\tilde{\Delta}^*(\mathbf{r}_1,\mathbf{r}_2)\tilde{u}(\mathbf{r}_2) &= E\tilde{v}(\mathbf{r}_1), \end{aligned} \tag{1}$$

where $H_e(\mathbf{r}_1)=-\hbar^2\nabla^2/2m+V(\mathbf{r}_1)-\mu$ is an electronic Hamiltonian and μ is the chemical potential. $\tilde{\Delta}(\mathbf{r}_1,\mathbf{r}_2)$ is the pair potential, $\tilde{u}(\mathbf{r}_1)$ and $\tilde{v}(\mathbf{r}_1)$ are the wave functions for the electronlike and holelike components of a quasiparticle,

$$\psi(\mathbf{r}_1) = \begin{pmatrix} \tilde{u}(\mathbf{r}_1) \\ \tilde{v}(\mathbf{r}_1) \end{pmatrix}. \tag{2}$$

The pair potential $\tilde{\Delta}(\mathbf{r}_1,\mathbf{r}_2)$ is a function of the position coordinates $\mathbf{r}_1$ and $\mathbf{r}_2$, and can be transformed to

$$\bar{\Delta}(\mathbf{R},\mathbf{r}) = \tilde{\Delta}(\mathbf{r}_1,\mathbf{r}_2), \tag{3}$$

with $\mathbf{R}=\mathbf{r}_1-\mathbf{r}_2$ and $\mathbf{r}=(\mathbf{r}_1+\mathbf{r}_2)/2$. The Fourier transform of $\bar{\Delta}(\mathbf{R},\mathbf{r})$ is

$$\Delta_{\mathrm{FT}}(\mathbf{k},\mathbf{r}) = \int d\mathbf{R}e^{-i\mathbf{k}\cdot R}\bar{\Delta}(\mathbf{R},\mathbf{r}). \tag{4}$$

Using the quasiclassical approximation, the pair potential $\Delta_{\mathrm{FT}}(\mathbf{k},\mathbf{r})$ is aproximated by

$$\Delta_{\mathrm{FT}}(\mathbf{k},\mathbf{r}) = \Delta(\hat{\mathbf{k}},\mathbf{r}), \tag{5}$$

where $\hat{\mathbf{k}}=\mathbf{k}/|\mathbf{k}|$ is a unit wave vector. Using $\Delta(\hat{\mathbf{k}},\mathbf{r})$, the BdG equations are approximated as

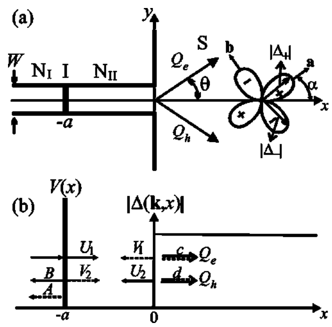

FIG. 1. (a) The point contact *NINS* junction. The insulating barrier is located at $x=-a$ and the *NIN* region is a single mode quantum wire with width W, the pair potential, Δ, in the normal metal is zero and in the superconductor region depends on θ; the axes a and b are along the a and b axes of the CuO_2 plane. For a d-symmetry, Δ is modeled as $\Delta(\theta)=\Delta_0\cos(2\theta-2\alpha)$. Two types of quasiparticles, Q_e and Q_h, are scattered at the N_{II}-S interface by the pair potentials Δ_+ and Δ_-, respectively. For Q_e, $\Delta(\theta)_+=\Delta_0\cos(2\theta-2\alpha)$ and for Q_h, $\Delta(\theta)_-=\Delta_0\cos(2\theta+2\alpha)$. The cones o lobes $(+)$ and $(-)$ represents the pair potentials $\Delta(\theta)_+$ and $\Delta(\theta)_-$, respectively. (b) Schematic energy diagram for the potentials and scattering processes. The solid and dashed lines represent the electron and the holelike components of a quasiparticle, respectively.

$$H_e(\mathbf{r})u_{\mathbf{k}}(\mathbf{r})+\Delta(\hat{\mathbf{k}},\mathbf{r})v_{\mathbf{k}}(\mathbf{r})=Eu_{\mathbf{k}}(\mathbf{r}), \tag{6}$$

$$-H_e^*(\mathbf{r}_1)v_{\mathbf{k}}(\mathbf{r})+\Delta^*(\hat{\mathbf{k}},\mathbf{r})u_{\mathbf{k}}(\mathbf{r})=Ev_{\mathbf{k}}(\mathbf{r}). \tag{7}$$

We focus in the rest of the paper on cuprate superconductor junctions. It is supposed that the quasiparticle moves on the CuO_2 plane with the a and b axes in the x-y plane; the interfaces are normal to the x-axis and the *NIN* region has a width W in the y direction, as indicated in Fig. 1. The insulating barrier is modeled by a delta function, $V(x)=U_0\delta(x+a)$ and the pair potential by $\Delta(\hat{\mathbf{k}},\mathbf{r})=\Theta(x)\Delta(\hat{\mathbf{k}})$, where $\Theta(x)$ is the Heaviside function. The solutions to the BdG equations in the N_I, N_{II} and in the superconducting regions are, respectively,

$$\psi_{N_I}=\left[\begin{pmatrix}1\\0\end{pmatrix}e^{ik_1^+x}+A\begin{pmatrix}0\\1\end{pmatrix}e^{ik_1^-x}+B\begin{pmatrix}1\\0\end{pmatrix}e^{-ik_1^+x}\right]\phi_1(y), \tag{8}$$

$$\psi_{N_{II}}=\left[U_1\begin{pmatrix}1\\0\end{pmatrix}e^{ik_1^+x}+U_2\begin{pmatrix}1\\0\end{pmatrix}e^{-ik_1^+x}+V_1\begin{pmatrix}0\\1\end{pmatrix}e^{ik_1^-x}+V_2\begin{pmatrix}0\\1\end{pmatrix}e^{-ik_1^-x}\right]\phi_1(y), \tag{9}$$

$$\psi_S=\int_{-\infty}^{\infty}ds\left[c(s)\begin{pmatrix}u_0^+(s)e^{i\varphi_+(s)/2}\\v_0^+(s)e^{-i\varphi_+(s)/2}\end{pmatrix}e^{ik_+^+(s)x}+d(s)\begin{pmatrix}v_0^-(s)e^{i\varphi_-(s)/2}\\u_0^-(s)e^{-i\varphi_-(s)/2}\end{pmatrix}e^{-ik_-^-(s)x}\right]\varphi_s(y), \tag{10}$$

with

$$\phi_1(y)=\sqrt{\frac{2}{W}}\sin\left[\frac{\pi}{W}\left(y+\frac{W}{2}\right)\right]\Theta\left(\frac{W}{2}-|y|\right),\qquad \varphi_s(y)=\frac{e^{isy}}{\sqrt{2\pi}}, \tag{11}$$

$$u_0^\pm(s)=\sqrt{\frac{1}{2}\left[1+\frac{\Omega_\pm(s)}{E}\right]},\quad v_0^\pm(s)=\sqrt{\frac{1}{2}\left[1-\frac{\Omega_\pm(s)}{E}\right]}, \tag{12}$$

$$\Omega_\pm(s)=\sqrt{E^2-|\Delta_\pm(s)|^2}. \tag{13}$$

$k_1^\pm$ are the electrons $(+)$ and holes $(-)$ wave numbers in the wire, which are functions of the energy E of the incoming electrons from region I; $k_+^+(s)$ and $k_-^-(s)$ are the wave numbers for the quasiparticles Q_e and Q_h, respectively (see Fig. 1) and depend on the wave number along the y axis, defined by s. The wave numbers are given by

$$k_1^\pm=\sqrt{k_1^2\pm\frac{2mE}{\hbar^2}},\quad k_1=\sqrt{k_F^2-\frac{\pi^2}{W^2}},\qquad k_\pm^\pm(s)=\sqrt{k(s)^2\pm\frac{2m\Omega_\pm(s)}{\hbar^2}},\quad k(s)=\sqrt{k_F^2-s^2}. \tag{14}$$

Since the quasiparticles Q_e and Q_h have different wave vectors, they undergo different effective pair potentials Δ_+ and Δ_-,

$$\Delta_\pm(s)=\Delta(\pm k_\pm^\pm\hat{\imath}+s\hat{\jmath})\equiv|\Delta_\pm|e^{i\varphi_\pm}, \tag{15}$$

where φ_+ and φ_- are the phases of the effective pair potentials Δ_+ and Δ_-, respectively. For a d-symmetry $\Delta_\pm=\Delta_0\cos[2(\theta\mp\alpha)]$, α is the angle between the (100) axis of the superconductor and the normal to the interface, and $\theta=\sin^{-1}(s/k_F)$ [cf. Fig. 1(a)]. Experimentally the angle α can be changed in angle-resolved ZBCP measurements of ramp-edge tunnel junctions with different crystal interface boundary angles.[14] In these experiments the width of the contact is reduced by using a focused-ion beam technique. From the measurements it is concluded that, as the width is reduced, the relative ZBCP height decreases, indicating that Andreev reflections decrease. The system illustrated in Fig. 1 can be materialized experimentally in a similar way if we add a defect or impurity at a distance a of the interface; this defect can be modeled as an insulating barrier.

To simplify the discussion, all the evanescent modes have been neglected. This approximation is justified because for $\pi<Wk_F<2\pi$ the narrow wire has a single mode and the energy of evanescent modes is well above the Fermi energy.[18,23] One finds A, B, U_1, U_2, V_1, V_2, c, and d using boundary conditions in $x=-a$ and $x=0$. Details are given in the Appendix. The electron-electron and electron-hole reflection coefficients are, respectively,

$$R_e=\left|\frac{h}{g}\right|^2,\quad R_h=\left|\frac{2F_3}{g}\right|^2, \tag{16}$$

$$g = (1 + Z^2)[(1 + F_1)^2 - F_2F_3] + Z^2[(1 - F_1)^2 - F_2F_3]e^{-2i(k_+ - k_-)a} + Z[1 - F_1^2 + F_2F_3][Z(e^{2ik_-a} + e^{-2ik_+a}) + i(e^{-2ik_+a} - e^{2ik_-a})], \quad (17)$$

$$h = (F_1^2 - F_2F_3 - 1)[Z^2e^{2i(k_+ + k_-)a} - (1 - iZ)^2] - Z(Z + i)[2F_1(e^{2ik_+a} - e^{2ik_-a}) + (1 + F_1^2 - F_2F_3)(e^{2ik_+a} + e^{2ik_-a})], \quad (18)$$

$$F_i = \frac{4}{\pi^2\sqrt{\gamma_F^2 - 1}}\int_{-\gamma_F}^{\gamma_F} dq \frac{\sqrt{\gamma_F^2 - q^2}}{(1 - q^2)^2}\cos^2\left(\frac{\pi q}{2}\right) f_i(q), \quad (19)$$

$$f_1 = \frac{1 + \Gamma_+\Gamma_- e^{-i(\varphi_+ - \varphi_-)}}{1 - \Gamma_+\Gamma_- e^{-i(\varphi_+ - \varphi_-)}}, \quad f_2 = \frac{2\Gamma_- e^{i\varphi_-}}{1 - \Gamma_+\Gamma_- e^{-i(\varphi_+ - \varphi_-)}},$$

$$f_3 = \frac{2\Gamma_+ e^{-i\varphi_+}}{1 - \Gamma_+\Gamma_- e^{-i(\varphi_+ - \varphi_-)}}, \quad (20)$$

$$\Gamma_\pm = \frac{v_0^\pm}{u_0^\pm}, \quad \gamma_F = \frac{k_F W}{\pi} \quad \text{and } Z = \frac{k_F U_0}{2E_F\sqrt{1 - \gamma_F^{-2}}}. \quad (21)$$

III. DIFFERENTIAL CONDUCTANCE

The differential conductance has been calculated by using the BTK model[30] for anisotropic superconductors.[3–6,8,29] For this calculation the electron-electron and electron-hole reflection coefficients are used. This result can be contrasted with those found from Green's functions calculations[31] for charge transport in diffusive normal metal/unconventional singlet superconductor contacts. For the ballistic limit the authors reproduced the generalized conductance obtained with the BTK model for anisotropic superconductors.[3,6] Using this model, the normalized differential conductance, G_R, at $T=0$ K is calculated from

$$G_R(eV) = \left.\frac{G_S(E)}{G_N}\right|_{E=eV} \quad (22)$$

$$= \frac{[(1 + F_0)^2 + 4Z^2][1 - R_e(eV) + R_h(eV)]}{4F_0}, \quad (23)$$

where G_N is the conductance when $\Delta=0$ and $a=0$. F_0 is defined by (19) with $f_i=1$ and the reflection coefficients are evaluated in $E=eV$, where V is the voltage.

Figures 2 and 3 show the differential conductance for s symmetry ($\Delta_+=\Delta_-=\Delta_0$) and $d_{x^2-y^2}$-symmetry ($\Delta_+=\Delta_-=\Delta_0\cos 2\theta$). When $a=0$ (*NIS* point contact), our results agree with Ref. 18. For $a\neq 0$ and symmetry s, subgap resonances appear in the differential conductance and their number increases with a. When Z decreases, it can be seen that the numbers and positions of the resonances remain unaltered; the peaks are just broader. For $d_{x^2-y^2}$-symmetry the number of peaks and their positions are similar to the s symmetry case, except that for a fixed Z value the width of the peak is greater.

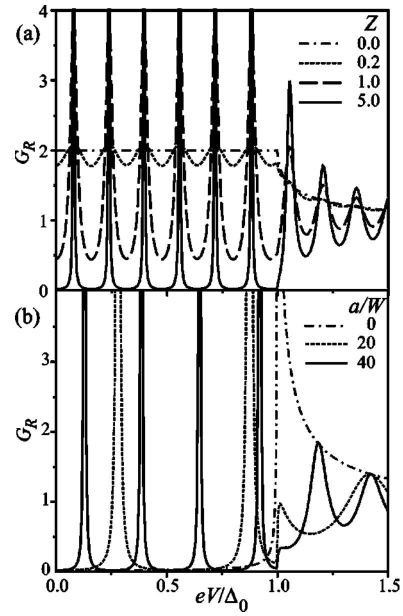

FIG. 2. Differential conductance for s-symmetry. (a) Different values of Z with $a=63W$; (b) different values of a with $Z=5$. In both cases $k_FW=1.7$.

Figure 4 exhibits the differential conductance for $\alpha=\pi/4$ (d_{x-y}-symmetry, $\Delta_-=-\Delta_+=\Delta_0\sin 2\theta$). ZBCP does not appear because the Andreev reflections are zero. In the last case the wave functions in the channel are a superposition of two plane waves with wave numbers $k_y=\pm\pi/W$. Each wave experiences a pair potential phase 0 and π, respectively, and therefore the Andreev reflection coefficient $a(\theta)$ [$R_h(\theta)=|a(\theta)|^2$] for each wave is outphased in π, therefore the waves of the reflected holes interfere destructively and the

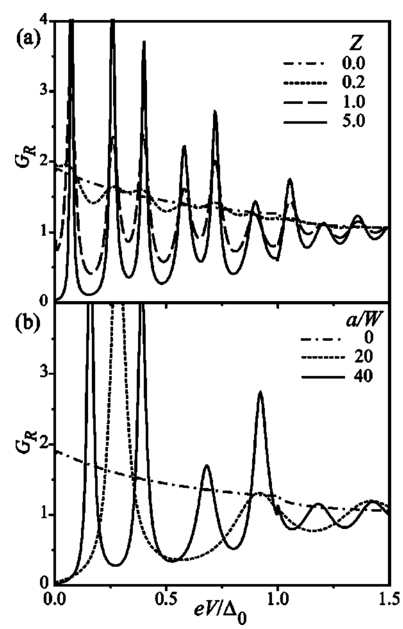

FIG. 3. Same as in Fig. 2 for $\alpha=0$ ($d_{x^2-y^2}$-symmetry).

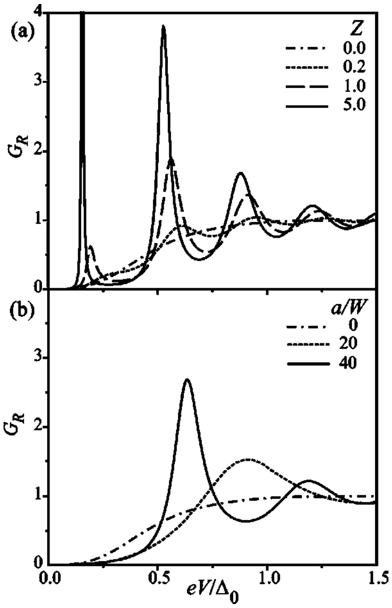

FIG. 4. Same as in Fig. 2 for $\alpha = \pi/4$ (d_{x-y}-symmetry).

Andreev reflections vanish. In relation with the d_{x-y}-symmetry the number of resonances decrease compared with the s and $d_{x^2-y^2}$-symmetries. Additionally, when Z decreases, the number of the resonances is constant, the peak broadens and its position is smoothly shifted to the right.

The subgap resonances in the differential conductance are a direct consequence of the quasibound states formed inside the energy gap. The energies and lifetimes of these quasibound states are given by the poles of the current transmission amplitude. Setting $g=0$ in Eq. (17) one finds these poles. A complex energy, $E=E_n+iE_I$, is required in order to solve this equation, where E_R is the position of resonance and $\hbar/(2|E_I|)$ is the lifetime of the quasibound states.

For s or $d_{x^2-y^2}$-symmetries the resonance positions E_n are given by

$$E_n = E_0(n\pi - \phi), \quad n = 1,2,\ldots, \tag{24}$$

and for d_{xy}-symmetry they are determined from

$$E_n = E_0(2n\pi - \phi'), \quad n = 1,2,\ldots. \tag{25}$$

In these equations

$$E_0 = \frac{E_F}{ak_F}\sqrt{1-\gamma_F^{-2}} \tag{26}$$

and ϕ,ϕ' are phases that depend on Z, a, and E. Therefore, the number of resonances with $E < \max(\Delta)$ for s- or $d_{x^2-y^2}$-symmetries are approximately twice the corresponding number of a d_{xy}-symmetry. This is due to the fact that in the case of a d_{xy}-symmetry the Andreev reflection is zero. The quantization of the quasibound states occurs when the quasiparticles travel in a round trip a distance equal to $2a$ in the x direction and $E_n \propto 2n\pi/2a$; see Fig. 5(a). In the case of s- or $d_{x^2-y^2}$-symmetries the quasiparticles complete a round trip when they travel a distance $4a$ along the x direction and $E_n \propto 2n\pi/4a$, as illustrated in Fig. 5(b). One concludes that in this case the number of quasibound states is approximately twice the corresponding number for the d_{x-y} symmetry.

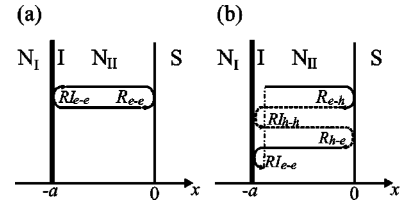

FIG. 5. Illustration of quasiparticle scattering processes that follow round trips: (a) the quasiparticle is reflected as an electron in $x=0$ and $x=-a$; (b) the quasiparticle is reflected as a hole in $x=0$, reflected as a hole in $x=-a$, reflected as an electron in $x=0$ and finally reflected as an electron in $x=-a$.

In order to determine the lifetime of the quasibound states, a semiclassical analysis will be used. The lifetime τ is defined as the time that a quasiparticle in the N_{II} region requires to "escape" toward the N_{I} or S region. For s or $d_{x^2-y^2}$-symmetries, a quasiparticle employs a time T for a round trip given by

$$T = \frac{4a}{\hbar k_{0F1}/m} = \frac{2\hbar d}{E_F\sqrt{1-\gamma_F^{-2}}}, \tag{27}$$

where $d=\pi a/w$. If N is the number of closed trips during which the probability that the quasiparticle still remains within the N_{II} region has decreased to $1/e$, the lifetime can be written as

$$\tau = TN, \tag{28}$$

where N is obtained from

$$(R_{e\text{-}h}RI_{h\text{-}h}R_{h\text{-}e}RI_{e\text{-}e})^N = 1/e, \tag{29}$$

with $R_{e\text{-}h}$, $R_{h\text{-}e}$ the electron-hole and hole-electron reflection coefficients, respectively, for $Z=0$ (point contact NS) and $RI_{e\text{-}e}$, $RI_{h\text{-}h}$ the electron-electron and hole-hole reflection coefficients, respectively, for an insulating barrier (IN). The expression $R_{e\text{-}h}RI_{h\text{-}h}R_{h\text{-}e}RI_{e\text{-}e}$ is the probability that the quasiparticle still remains in the N_{II} region in one round trip, see Fig. 5(b). From Eqs. (27), (28), and (29) one finds that the lifetime is given by

$$\tau = -\frac{\hbar d}{E_F\sqrt{1-\gamma_F^{-2}}}\frac{1}{\ln[Z^2R_{e\text{-}h}/(1+Z^2)]}, \tag{30}$$

where we have used the facts that $R_{e\text{-}h}=R_{h\text{-}e}$ and $RI_{e\text{-}e}=RI_{h\text{-}h}=Z^2/(1+Z^2)$. Equation (30) is like the one found for *NINS* junctions with s-symmetry.[24] Similarly, for the d_{xy}-symmetry N is obtained from

$$(R_{e\text{-}e}RI_{e\text{-}e})^N = 1/e, \tag{31}$$

with $R_{e\text{-}e}$ the electron-electron reflection coefficient for $Z=0$. The expression $R_{e\text{-}e}RI_{e\text{-}e}$ is the probability that the quasiparticle still remains in the N_{II} region after one round trip, see Fig. 5(a), From Eqs. (27), (28), and (31) one finds that the lifetime is given by

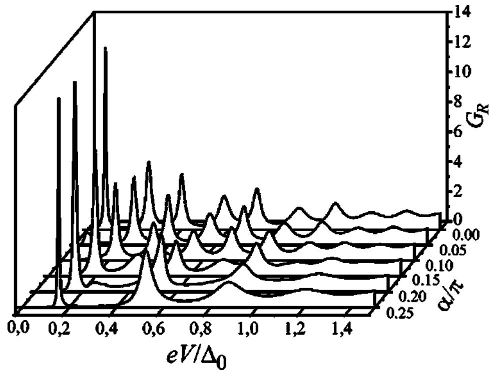

FIG. 6. Differential conductance for d-symmetry, $\Delta_\pm = \Delta_0 \cos[2(\theta \mp \alpha)]$ with $Z=5$, $a=63W$, $k_F W=1.7$ and different values of α.

$$\tau = -\frac{\hbar d}{E_F\sqrt{1-\gamma_F^{-2}}}\frac{1}{\ln[Z^2 R_{e\text{-}e}/(1+Z^2)]}. \qquad (32)$$

For the case of s-symmetry and $E<|\Delta|$, $R_{e\text{-}h}=1$. Therefore the lifetime increases with Z and tends to infinity for $Z \gg 1$, while the resonance width, $2|E_I| \approx \hbar/\tau \to 0$, as it is observed in Fig. 2. For $d_{x^2-y^2}$-symmetry the quasiparticle transmission coefficient is finite for $E<\Delta_0$ due to the anisotropy of the pair potential, $R_{e\text{-}h}<1$, and the lifetime increases with Z but is finite for $Z \gg 1$. This is observed in the width of the resonances shown in Fig. 3. For the d_{xy}-symmetry the behavior of the lifetime and the width of the resonances are similar to the case of $d_{x^2-y^2}$-symmetry, see Fig. 4. For all cases, with $E>\Delta_0$, the reflection coefficients are always less than one, the lifetimes decrease and the widths of the resonances increase.

Figure 6 shows how the differential conductance G_R evolves for different values of α between 0 and $\pi/4$. Notice that some peaks begin to decrease and vanish for $\alpha \approx 0.20\pi$. This happens because the Andreev reflections decrease and the electron-electron reflection increases. For $\alpha = \pi/4$ the Andreev reflections are zero and one has the conductance for d_{xy}-symmetry. Similarly, the resonances energy values move toward the left as α increases due to a change of the phase ϕ in the solution of the equation $g=0$.

Finally, it is interesting to note that if one considers the p-type symmetry, because the Andreev reflection is present for a single normal mode,[20] the number of resonances must be similar to the s and $d_{x^2-y^2}$-cases, although a zero voltage peak is expected. This will be an interesting topic to explore further.

IV. CONCLUSIONS

Our results show that at *NINS* point contacts the differential conductance have resonances due to quasibound states. The number of resonances depends on the symmetry of the order parameter, in contrast to a *NINS* junction. In the latter case only the position of the resonances changes with the symmetry. The number of resonances with $E<\max(\Delta)$ (subgap resonances), for s- or $d_{x^2-y^2}$-symmetries is approximately twice the corresponding number for the d_{xy}-symmetry. When α changes from 0 to $\pi/2$ some peaks disappear because the Andreev reflection vanishes.

In the case of s-symmetry, the lifetime of quasibound states increases with the insulating barrier strength and is infinite for $Z \gg 1$. In contrast, for a d-symmetry the lifetime increases with Z but is finite for $Z \gg 1$. This occurs because the quasiparticles transmission is different from zero for $E<\Delta_0$ in contrast to the case of s-symmetry, where the transmission is zero for $E<\Delta_0$. Therefore, the lifetime of the resonances decreases in d-symmetries and their width increases. The results obtained in this work can be used to find the symmetry of high temperature superconductors in experiments of the type carried out in Ref. 14.

ACKNOWLEDGMENT

The authors have received support from División de Investigaciones de la Universidad Nacional de Colombia sede Bogotá.

APPENDIX: REFLECTION COEFFICIENTS

The boundary conditions for the wave function of a quasiparticle in $x=-a$, are

$$\Psi_{N_{\rm I}}(-a) = \Psi_{N_{\rm II}}(-a),$$
$$\left.\frac{d\Psi_{N_{\rm I}}(x)}{dx}\right|_{x=-a} = \left.\frac{d\Psi_{N_{\rm II}}(x)}{dx}\right|_{x=-a} - 2m\frac{U_0}{\hbar^2}\Psi_{N_{\rm I}}(-a), \qquad ({\rm A1})$$

from them we obtain

$$e^{-ik_1^+ a} + Be^{ik_1^+ a} = U_1 e^{ik_1^+ a} + U_2 e^{-ik_1^+ a}, \qquad ({\rm A2a})$$

$$Ae^{ik_1^- a} = V_1 e^{ik_1^- a} + V_2 e^{-ik_1^- a}, \qquad ({\rm A2b})$$

$$e^{-ik_1^+ a}(2iZ-1) + Be^{ik_1^+ a}(1+2iZ) = U_1 e^{ik_1^+ a} - U_2 e^{-ik_1^+ a}, \qquad ({\rm A2c})$$

$$Ae^{ik_1^- a}(1-2iZ) = V_1 e^{ik_1^- a} - V_2 e^{-ik_1^- a}. \qquad ({\rm A2d})$$

From the continuity conditions for the wave function and its first derivative, in $x=0$,

$$\Psi_{N_{\rm II}}(0) = \Psi_S(0), \qquad \left.\frac{d\Psi_{N_{\rm II}}(x)}{dx}\right|_{x=0} = \left.\frac{d\Psi_S(x)}{dx}\right|_{x=0}, \qquad ({\rm A3})$$

we have that

$$[U_1+U_2]\phi_1(y) = \int_{-\infty}^{\infty} ds\big[c(s)u_0^+(s)e^{i\varphi_+(s)/2} + d(s)v_0^-(s)e^{i\varphi_-(s)/2}\big]\varphi_s(y), \qquad ({\rm A4a})$$

$$[V_1+V_2]\phi_1(y) = \int_{-\infty}^{\infty} ds\big[c(s)v_0^+(s)e^{-i\varphi_+(s)/2} + d(s)u_0^-(s)e^{-i\varphi_-(s)/2}\big]\varphi_s(y), \qquad ({\rm A4b})$$

$$k_1[U_1 - U_2]\phi_1(y) = \int_{-\infty}^{\infty} dsk(s)\Big[c(s)u_0^+(s)e^{i\varphi_+(s)/2} - d(s)v_0^-(s)e^{i\varphi_-(s)/2}\Big]\varphi_s(y), \quad \text{(A4c)}$$

$$k_1[V_1 - V_2]\phi_1(y) = \int_{-\infty}^{\infty} dsk(s)\Big[c(s)v_0^+(s)e^{-i\varphi_+(s)/2} + d(s)u_0^-(s)e^{-i\varphi_-(s)/2}\Big]\varphi_s(y). \quad \text{(A4d)}$$

We have used the Andreev approximation in the boundary conditions for the first derivative of the wave function, $k_1^+ = k_1^- = k_1$ and $k_+^+(s) = k_-^-(s) = k(s)$. Multiplying Eqs. (A4) by $\varphi_{s'}(y)dy$ and integrating over y we obtain

$$[U_1 + U_2]P_1(s) = c(s)u_0^+(s)e^{i\varphi_+(s)/2} + d(s)v_0^-(s)e^{i\varphi_-(s)/2}, \quad \text{(A5a)}$$

$$[V_1 + V_2]P_1(s) = c(s)v_0^+(s)e^{-i\varphi_+(s)/2} + d(s)u_0^-(s)e^{-i\varphi_-(s)/2}, \quad \text{(A5b)}$$

$$k_1[U_1 - U_1]P_1(s) = k(s)\Big[c(s)u_0^+(s)e^{i\varphi_+(s)/2} - d(s)v_0^-(s)e^{i\varphi_-(s)/2}\Big], \quad \text{(A5c)}$$

$$k_1[V_1 - V_2]P_1(s) = k(s)\Big[c(s)v_0^+(s)e^{-i\varphi_+(s)/2} - d(s)u_0^-(s)e^{-i\varphi_-(s)/2}\Big], \quad \text{(A5d)}$$

where

$$P_1(s) = \int_{-\infty}^{\infty} dy\,\phi_1(y)\varphi_s(y) = \frac{2}{W}\sqrt{\frac{\pi}{W}}\frac{\cos(sW/2)}{\pi^2/W^2 - s^2}. \quad \text{(A6)}$$

From the normalization conditions

$$\int_{-\infty}^{\infty} dy\,\varphi_{s'}^*(y)\varphi_s(y) = \delta(s - s'), \quad \int_{-\infty}^{\infty} dy\,\phi_1^*(y)\phi_1(y) = 1, \quad \text{(A7)}$$

the function $P_1(s)$ has the following property:

$$\int_{-\infty}^{\infty} dsP_1^*(s)P_1(s) = 1. \quad \text{(A8)}$$

From Eqs. (A2) and (A5) we obtain the following equations for A and B:

$$\left(1 - iZ(1 + e^{2ik_1^-a}) + \Big[1 - iZ(1 - e^{2ik_1^-a})\Big]\frac{k(s)f_1(s)}{k_1}\right)P_1(s)A - \Big[1 + iZ(1 - e^{-2ik_1^+a})\Big]\frac{k(s)f_3(s)}{k_1}P_1(s)B = \Big[1 - iZ(1 - e^{2ik_1^+a})\Big]\frac{k(s)f_2(s)}{k_1}P_1(s), \quad \text{(A9a)}$$

$$\Big[1 - iZ(1 - e^{2ik_1^-a})\Big]\frac{k(s)f_2(s)}{k_1}P_1(s)A - \left(\Big[1 + iZ(1 - e^{-2ik_1^+a})\Big]\frac{k(s)}{k_1}f_1(s) + 1 + iZ(1 + e^{-2ik_1^+a})\right)P_1(s)B = \Big[1 - iZ(1 - e^{2ik_1^+a})\Big]\frac{k(s)f_1(s)}{k_1}P_1(s) - \Big[1 - iZ(1 + e^{2ik_1^+a})P_1(s)\Big]. \quad \text{(A9b)}$$

Here the functions f_i, $i=1, 2, 3$, are defined by Eq. (20). Multipliying (A9) by $P_1^*(s)ds$, integrating over s and using (A8) we obtain a system of equations for A and B,

$$\Big\{1 - iZ(1 + e^{2ik_1^-a}) + \Big[1 - iZ(1 - e^{2ik_1^-a})\Big]F_1\Big\}A - \Big[1 + iZ(1 - e^{-2ik_1^+a})\Big]F_3B = \Big[1 - iZ(1 - e^{2ik_1^+a})\Big]F_2, \quad \text{(A10a)}$$

$$\Big[1 - iZ(1 - e^{2ik_1^-a})\Big]F_2A - \Big\{\Big[1 + iZ(1 - e^{-2ik_1^+a})\Big]F_1 + 1 + iZ(1 + e^{-2ik_1^+a})\Big\}B = \Big[1 - iZ(1 - e^{2ik_1^+a})\Big]F_1 - \Big[1 - iZ(1 + e^{2ik_1^+a})\Big], \quad \text{(A10b)}$$

where

$$F_i = \int_{-\infty}^{\infty} ds\frac{k(s)}{k_1}\frac{\pi}{W}\frac{4}{W^2}\frac{\cos^2(sW/2)}{(\pi^2/W^2 - s^2)^2}f_i(s).$$

Since the states that contribute to superconductivity are around the Fermi energy and in the Andreev approximation the magnitude of the wave vectors is k_F, the integrals over s between $-\infty$ to ∞ are approximated by $-k_F$ and k_F; with this, the functions F_i are written as

$$F_i \cong \int_{-k_F}^{k_F} ds\frac{k(s)}{k_1}\frac{\pi}{W}\frac{4}{W^2}\frac{\cos^2(sW/2)}{(\pi^2/W^2 - s^2)^2}f_i(s) = \frac{4}{\pi^2\sqrt{\gamma_F^2 - 1}}\int_{-\gamma_F}^{\gamma_F} dq\frac{\sqrt{\gamma_F^2 - q^2}}{(1 - q^2)^2}\cos^2\left(\frac{\pi q}{2}\right)f_i(q) \quad \text{(A11)}$$

with

$$q = \frac{Ws}{\pi}, \quad \gamma_F = \frac{Wk_F}{\pi}. \quad \text{(A12)}$$

The solutions for Eqs. (A10) are given by

$$A = \frac{2F_3}{g} \quad \text{and } B = \frac{h}{g}, \quad \text{(A13)}$$

with g and h given by (17) and (18). Finally we obtain the reflection coefficients electron-electron (R_e) and electron-hole (R_h) as

$$R_e = |B|^2, \quad R_h = |A|^2. \tag{A14}$$

It is important to underline that in the normal region we have approximated to one mode only. If one takes into account all the possible modes, $n=1$ to $n=\infty$, one must determine the reflection amplitude in each mode for electrons, B_n, and holes, A_n. Instead of Eq. (A9b) one obtains one equation that is a linear combination of functions $P_n(s) = \int_{-\infty}^{\infty} dy\, \phi_n(y)\varphi_s(y)$ with coefficients A_n and B_n. To illustrate, let us assume that one has a N-N contact, $\Delta=0$ and $Z=0$. In a way similar to the case where one obtains the equations for A and B, one obtains

$$\sum_{n=1}^{\infty} B_n P_n(s)(k(s) + k_n) = (k_1 - k(s))P_1(s). \tag{A15}$$

Multipliying by $P_n^*(s)ds$, integrating in s we obtain the system of equations

$$\sum_{n=1}^{\infty} B_n H_{mn} + k_m B_m = k_1 \delta_{1,m} - H_{m1}, \tag{A16}$$

with

$$H_{nm} = \int ds P_m^*(s) k(s) P_n(s). \tag{A17}$$

Equations (A16) are solutions to Eq. (A15) for all s only if one adds contributions from all the modes. Since this is not possible, the sum goes up to an appropiate n. This justifies the type of solution that one finds in Eqs. (A13), with first mode approximation. If one neglects modes with $n \geqslant 2$, one obtains from (A16),

$$B_1 = \frac{k_1 - H_{11}}{H_{11} + k_1}. \tag{A18}$$

This result is a particular case of (A13) ($B_1 \equiv B$) when $\Delta = 0$ and $Z=0$.

---

*Electronic address: jherreraw@unal.edu.co
†Electronic address: jvninoc@unal.edu.co
‡Electronic address: jjgiraldog@unal.edu.co

[1] C. C. Tsuei and J. R. Kirtley, Phys. Rev. Lett. **85**, 182 (2000).
[2] D. J. VanHarlingen, Rev. Mod. Phys. **67**, 515 (1995).
[3] Y. Tanaka and S. Kashiwaya, Phys. Rev. Lett. **74**, 3451 (1995).
[4] S. Kashiwaya and Y. Tanaka, Rep. Prog. Phys. **63**, 1641 (2000).
[5] S. Kashiwaya, Y. Tanaka, M. Koyanagi, H. Takashima, and K. Kajimura, Phys. Rev. B **51**, 1350 (1995).
[6] S. Kashiwaya, Y. Tanaka, M. Koyanagi, and K. Kajimura, Phys. Rev. B **53**, 2667 (1996).
[7] Y. S. Barash, A. A. Svidzinsky, and H. Burkhardt, Phys. Rev. B **55**, 15 282 (1997).
[8] M. B. Walker and P. Pairor, Phys. Rev. B **60**, 10 395 (1999).
[9] M. Covington, R. Scheuerer, K. Bloom, and L. H. Greene, Appl. Phys. Lett. **68**, 1717 (1996).
[10] L. Alff, H. Takashima, S. Kashiwaya, N. Terada, H. Ihara, Y. Tanaka, M. Koyanagi, and K. Kajimura, Phys. Rev. B **55**, R14 757 (1997).
[11] J. Y. T. Wei, N.-C. Yeh, D. F. Garrigus, and M. Strasik, Phys. Rev. Lett. **81**, 2542 (1998).
[12] M. Aprili, M. Covington, E. Paraoanu, B. Niedermeier, and L. H. Greene, Phys. Rev. B **57**, R8139 (1998).
[13] W. Wang, M. Yamazaki, K. Lee, and I. Iguchi, Phys. Rev. B **60**, 4272 (1999).
[14] I. Iguchi, W. Wang, M. Yamazaki, Y. Tanaka, and S. Kashiwaya, Phys. Rev. B **62**, R6131 (2000).
[15] J. Yang and C.-R. Hu, Phys. Rev. B **50**, 16 766 (1994).
[16] C.-R. Hu, Phys. Rev. Lett. **72**, 1526 (1994).
[17] Y. Tanaka and S. Kashiwaya, Phys. Rev. B **53**, 9371 (1996).
[18] Y. Takagaki and K. H. Ploog, Phys. Rev. B **60**, 9750 (1999).
[19] K. Tsuchikawa, N. Yoshida, Y. Tanaka, S. Kashiwaya, J. Inoue, and Y. Takagaki, Physica C **352**, 224 (2001).
[20] K. Tsuchikawa, N. Yoshida, Y. Tanaka, S. Kashiwaya, J. Inoue, and Y. Takagaki, Physica C **357**, 1588 (2001).
[21] Y. Tanaka and S. Kashiwaya, Phys. Rev. B **70**, 012507 (2004).
[22] Y. Tanaka, Y. Tanuma, K. Kuroki, and S. Kashiwaya, J. Phys. Soc. Jpn. **71**, 2102 (2002).
[23] S. Takahashi, T. Yamashita, and S. Maekawa, cond-mat/0401111.
[24] R. A. Riedel and P. F. Bagwell, Phys. Rev. B **48**, 15 198 (1993).
[25] S. H. Tessmer, D. J. VanHarlingen, and J. W. Lyding, Phys. Rev. Lett. **70**, 3135 (1993).
[26] W. L. McMillan, Phys. Rev. **175**, 559 (1968).
[27] W. J. Herrera and J. V. Niño, Phys. Status Solidi B **220**, 555 (2000).
[28] J. H. Xu, J. H. Miller, Jr., and C. S. Ting, Phys. Rev. B **53**, 3604 (1996).
[29] C. Bruder, Phys. Rev. B **41**, 4017 (1990).
[30] G. E. Blonder, M. Tinkham, and T. M. Klapwijk, Phys. Rev. B **25**, 4515 (1982).
[31] Y. Tanaka, Y. V. Nazarov, A. A. Golubov, and S. Kashiwaya, Phys. Rev. B **69**, 144519 (2004).